Determination of active sites during gasification of biomass char with CO_2 using temperature-programmed desorption. Part 2: Influence of ash components

Sonia Rincón Prat[b], Christoph Schneider[a,*], Thomas Kolb[a,c]

[a] *Karlsruhe Institute of Technology, Engler-Bunte-Institute, Fuel Technology, EBI-ceb, Engler-Bunte-Ring 3, 76131 Karlsruhe, Germany*
[b] *Universidad Nacional de Colombia, Departamento de Ingeniería Mecánica y Mecatrónica, Grupo de Investigación en Biomasa y Optimización Térmica de Procesos, BIOT, Carrera 30 No 45A-03, Bogotá, Colombia*
[c] *Karlsruhe Institute of Technology, Institute for Technical Chemistry, ITC-vgt, Hermann-von-Helmholtz-Platz 1, 76344 Eggenstein-Leopoldshafen, Germany*

Keywords:
Biomass char
Gasification kinetics
Surface chemistry
Temperature-programmed desorption
Active sites
Inorganic ash components
Catalytically active sites

A B S T R A C T

The present work is the second part of a study conducted with the aim to determine the amount of active sites present on the surface of a biomass char participating in the gasification reaction with CO_2 using the temperature programmed desorption (TPD) technique. In part 1, the methodology and experimental results during TPD of partially gasified samples of beech wood char (WC1600) using CO_2 as gasification agent are presented. This work focusses on the influence of the main inorganic ash components of WC1600 on the CO_2 and CO signals obtained during TPD of partially gasified char samples. Furthermore, an activated carbon with ash content lower than 1 wt-% is impregnated with Ca and K and partially gasified followed by a TPD analysis. CO_2 and CO signals obtained during TPD result from decomposition of oxygenated surface complexes and decomposition reactions of ash components. During gasification, three different kinds of sites are present on the surface of the char: stable, reactive and catalytically active sites. The latter are a measure of the catalytic influence of inorganic matter during char gasification. From the analysis of the TPD spectra, it can be concluded that gasification of WC1600 is dominated by the catalytic influence exerted by Ca and K. Formation of oxygenated surface complexes on WC1600 is limited, possibly due to the high temperature at which the sample was pyrolyzed (1600 °C). However, a direct correlation between specific conversion rate and the amount of reactive and catalytically active sites is developed from the experimental results, corrected by the contribution of ash decomposition.

1. Introduction

The knowledge of biomass char gasification kinetics is necessary for process and reactor design. It is the slowest reaction taking place inside the gasifier determining its size and the process conditions in the gasification plant. As char gasification is a heterogeneous gas–solid reaction, it is dependent not only on temperature and on concentration of gasifying agent but also on the origin and the physical and chemical characteristics of the solid char. Most of the studies concentrate on the determination of global formal kinetic parameters that are restricted to the raw material and the processing conditions and that do not take into account the change in specific conversion rate as the reaction proceeds [1–3]. Variation in specific conversion rate is considered by a structural term describing the change of physical char properties, i.e. the char surface [4]. Moreover, the great variety of experimental set-ups and conditions implemented during experimentation make the results on same raw materials difficult to compare. Studies on the intrinsic reaction rate and the derivation of kinetic expressions that lie on the fundamental mechanism of the char gasification reaction are limited. The most widely accepted mechanism for the gasification of char with CO_2 or H_2O is the oxygen exchange mechanism in which gasification takes place via formation and decomposition of carbon–oxygen intermediates [1,2]. From a fundamental point of view in a kinetic expression of carbon (or char) gasification, the specific conversion rate should be proportional to the surface concentration of the reactant gas (at constant temperature). Assuming constant partial pressure of the reactant gas (pseudo-zero-order reaction), the surface concentration of the gaseous reactant is described by the chemisorption isotherm which is proportional to the surface concentration of carbon atoms participating in the gasification reaction. The determination of these carbon atoms is still one of the current challenges in the study of the char gasification kinetics. Lizzio et al. [5] introduced the concept of reactive surface area

* Corresponding author.
E-mail addresses: slrinconp@unal.edu.co (S. Rincón Prat), ch.schneider@kit.edu (C. Schneider), thomas.kolb@kit.edu (T. Kolb).

as a measure of the amount of carbon atoms participating in the gasification reaction. They stated that during gasification the char surface contains stable C-O and unstable C(O) complexes formed on stable and reactive sites. The reactive surface area (RSA) is the number of carbon atoms which are able to form carbon oxygen intermediates (unstable C(O) complexes) and are decomposed subsequently to desorb as gaseous product.

The present work is the second part of a study aiming for a better understanding concerning the role of chemical properties of the char surface in the mechanism of biomass char gasification with CO_2. A methodology for measurement of stable C-O and unstable C(O) complexes based on the temperature-programmed desorption (TPD) technique proposed by Lizzio et al. [5] is applied using a beech wood biomass char. An analysis of the obtained CO and CO_2 spectra presented in part 1 [6] shows that the TPD signals are not only a result of decomposition of oxygenated surface complexes followed by desorption of gaseous products but also of decomposition of ash constituents, as both processes yield in oxygenated gases (CO and CO_2) during the desorption phase of TPD experiments [5,7].

Only little work concerning the analysis of released gases during TPD of coal or biomass char after gasification that considers the effect of ash components can be found in literature. In their work, Lizzio et al. [5] measured total and stable complexes using TPD experiments for partially gasified chars with different ash contents (bituminous coal char, polyvinylidene chloride (Saran) char and a Ca-loaded and demineralized lignite). For the quantification of the complexes, they only used the CO signal as they assumed that the CO_2 signal arises from decomposition reactions of ash, especially the decomposition of $CaCO_3$. Kyotani et al. [7] proposed in their study on the catalytic influence of mineral matter during gasification with H_2O of brown coal that H_2O, CO_2 and CO released during TPD, after partial gasification of the samples, is the consequence of the presence of Ca, Mg, Na and Fe. In another work, the same group [8] concludes that the mechanism responsible for the release of gas species detected in the TPD spectra is closely related to the catalytic activity of mineral matter during gasification. They state that the amount of oxygen contained in inorganic species and in carbon–oxygen complexes after gasification is a measure of carbon specific conversion rate. In the more recent works of Klose and Wölki [2] and Guizani et al. [9], who made TPD analysis of partially gasified biomass char samples using CO_2 or H_2O as gasifying agent, there is no mention of the possibility of ash decomposition reactions resulting in the release of CO_2 and CO during TPD.

Based on the conclusions presented in part 1 of this study [6] this paper concentrates on the analysis of TPD spectra of partially gasified beech wood char samples from the point of view of the influence of its ash components. First, a summary of relevant results presented in literature concerning desorption of oxygenated surface complexes and decomposition of ash components from biomass char and coal char that influence TPD spectra is presented. Then, experimental results of TPD of partially gasified samples of a low ash content commercial activated carbon impregnated with the main ash components of the beech wood char under study (Ca and K) is given. The findings are finally applied to the results of TPD spectra obtained for partially gasified samples presented in the first part of this study [6] and conclusions about the influence of decomposition of ash components in the TPD spectra and its relationship to the gasification process are drawn.

2. Literature review on TPD behavior of oxygen surface complexes and biomass ash components

2.1. Carbon oxygen surface complexes and their decomposition behavior during TPD

Carbon oxygen surface complexes are present in the form of oxygenated groups on the surface of carbon materials. They act not only as surface intermediates in gasification reactions (and other) but also determine the surface chemistry of the material, influencing its application as catalyst or as adsorbent, among others [10,11]. They form on the edges of the basal plane of the graphite layer of carbon materials where unsaturated carbon atoms are present and on defects, dislocations and discontinuities present on these basal planes [12]. Oxygen surface groups form acidic, basic or neutral structures that decompose during TPD at different temperature ranges yielding CO, CO_2 and H_2O. Fig. 1 shows the most common oxygenated groups found in carbon materials with their typical decomposition temperatures and the released gases during decomposition. Groups not shown in the figure like lactols, aldehydes, ketones and chromenes can also be present in low amounts [13,14]. Decomposition temperatures of oxygenated surface complexes are influenced by the structure of the carbon material, the heating rate and the experimental system [15]. Therefore, they appear in a wide interval during TPD. General trends show that the CO_2 releasing oxygen groups desorb in the lower temperature range (between 100 °C and 700 °C). Carboxylic anhydrides desorb yielding equimolar amounts of CO_2 and CO at intermediate temperatures (350 °C to 620 °C). Complexes releasing CO desorb at higher temperatures (550 °C to 1000 °C) [11]. According to Calo and Hall [16], oxygenated groups yielding CO_2 (e.g. carboxylic acid, anhydrides and lactones) are formed preferably in the mesopores of the carbon structure because of their large size. At the same time, smaller structures that yield CO during desorption (e.g. carbonyl, ketone and ethers) are formed in the micropores.

During TPD, CO and CO_2 signals appear overlapped. Thus, TPD

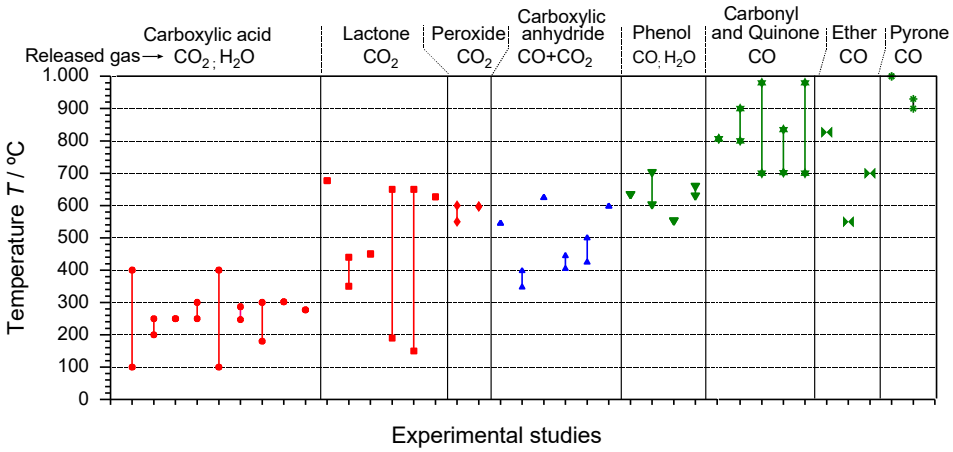

Fig. 1. Decomposition temperatures of different functional groups present as oxygenated surface complexes on carbon materials. Summarized from data compiled by Ishii and Kyotani [20] and Tremblay et al. [14].

peaks can be assigned to different functional groups. The assignment is often accompanied by other techniques like acid-base titration, infrared spectroscopy (FT-IR) and X-ray photoelectron spectroscopy (XPS) [17–19]. Moreover, the desorption behavior of complexes adsorbed in the micropores can be influenced by its location within the pore and the neighboring complexes. As pointed out by Calo and Hall [16], CO, which is the primary desorption product of the complexes in micropores, has a high probability of interacting with other complexes and free sites on the surface undergoing a secondary oxidation reaction to form CO_2. The reaction takes place at intermediate temperatures. At low temperatures (lower than 400 °C), C(O) complexes are inactive whereas at very high temperatures, the equilibrium of the oxidation reaction is shifted to the CO side. The authors state that CO_2 formation from secondary oxidation of CO can be either minimized by using low heating rates during TPD (in their work lower than 20 K/min) as the concentration of evolved CO within the pores remains low. On the other hand, very high heating rates should be used (higher than 500 K/min) in order to minimize the residence time of released CO within the micropores.

Figueiredo et al. [10] studied the formation of oxygenated surface complexes based on the CO and CO_2 evolution during TPD of activated carbon from coconut shell char partially oxidized in 5% O_2 in N_2 at 425 °C. TPD experiments were performed using a heating rate of 5 K/min in He atmosphere. They concluded that the evolving CO_2 originates from desorption of carboxylic anhydrides and lactones with maxima at 603 °C and 631 °C respectively. No evolution of CO_2 is observed at lower temperatures. The evolution of CO is attributed to desorption of carboxylic anhydrides (accompanied by CO_2 evolution), phenols and carbonyl/quinones with maxima at 603 °C, 674 °C and 821 °C respectively. Szymanski et al. [13] conducted deconvolution of the CO_2 and CO signals of TPD profiles of demineralized commercial activated carbon oxidized with nitric acid. The obtained CO_2 profile is composed of five peaks, although two of them with maxima at 290 °C and 430 °C show the higher contributions. This signal is attributed to the decomposition of carboxylic compounds at lower temperatures and to anhydrides, lactones or lactols at higher temperatures followed by desorption of CO_2. The CO profile shows the presence of four peaks in the temperature range between 250 °C and 700 °C which are attributed to the decomposition of carbonyl and carboxylic groups at lower temperatures and phenol and quinone groups at higher temperatures. Zhou et al. [18] studied the formation of oxygenated surface groups on a carbon nanofiber submitted to different heat treatments including oxidation in air and O_2 at temperatures between 400 °C and 600 °C. They characterized the surface oxygen complexes by deconvolution of TPD spectra together with FT-IR and XPS measurements. TPD was performed under Ar atmosphere at 10 K/min until 1000 °C. Additionally to the surface complexes already determined by other authors they attribute CO peaks obtained at low temperatures (lower than 300 °C) to adsorbed CO. Samples that were submitted to high temperatures under Ar atmosphere (900 °C and 1700 °C) before oxidation showed a CO_2 peak at high temperatures (above 800 °C) that could not be identified and is referred to as desorbed unknown group. They also conclude that high temperature treatment (oxidation at 600 °C and heating in Ar at 1700 °C) causes a higher degree of graphitization of the carbon nanofibers and consequently, a decrease in number of surface oxygenated groups.

2.2. Decomposition behavior of biomass ash components during TPD

Biomass ash is composed of high concentrations of alkali and alkaline earth metallic species (AAEM), mainly K and Ca together with small fractions of Na and Mg. Si, Al and Fe are also present in ash whereas the highest contribution is exerted by Si [21–23]. Studies on decomposition of ash components are based on TPD, differential scanning calorimetry (DSC), thermogravimetric analysis (TGA) and in some cases X-ray diffraction measurements. Experimental work is made on the more representative components of char and/or biomass char ashes and their mixtures. Following a summary of the main findings about the decomposition behavior during TPD of individual ash components and biomass char ash is presented.

2.2.1. Decomposition of individual components

After gasification, AAEM are generally present as carbonates [23,24]. During TPD in inert atmosphere, $CaCO_3$ decomposes according to the decarboxylation reaction in solid state (R6), yielding CO_2 in the temperature interval between 600 and 800 °C [25–28]. Formation of CO according to (R7) takes place to a very small extent at slightly lower temperatures [29].

Regarding K_2CO_3 its decomposition according to reaction (R8) takes place at temperatures above 900 °C–1150 °C [30,31]. Arvelakis et al. [31] state that this reaction occurs after melting of K_2CO_3 at temperatures near 900 °C. However, contrary to the findings about the reaction of $CaCO_3$ in presence of C, Kopyscinski et al. [32] found that reaction of K_2CO_3 according to reaction (R9) predominates as only CO was detected in their experiments in TGA in N_2 atmosphere. This reaction takes place at temperatures above 700 °C [32]. $CaCO_3$ and K_2CO_3 decomposition (according to reactions (R6) and (R8)) is inhibited by the presence of CO_2 [27,29,33,34].

$$CaCO_3 \leftrightarrows CaO + CO_2 \quad \text{(R6)}$$

$$CaCO_3 + C \rightarrow CaO + 2CO \quad \text{(R7)}$$

$$K_2CO_3 \leftrightarrows K_2O + CO_2 \quad \text{(R8)}$$

$$K_2CO_3 + 2C \rightarrow 2K + 3CO \quad \text{(R9)}$$

During heat treatment, gaseous K formed after decomposition of K_2O (generated according to R8) can escape the sample [35]. Zhao et al. [35] observed in samples of K_2CO_3 submitted to heating in a fixed bed reactor at 900 °C during 120 min under N_2 atmosphere a loss of 20% of the original K. Nzihou et al. [23] indicate that alkali compounds tend to suffer evaporative losses during pyrolysis and gasification conditions due to their high vapor pressures.

Decomposition reactions of silicon take place in presence of C with CO evolution by different reactions yielding SiO, SiC and/or Si. According to Biernacki and Wotzak [36] and Henderson and Tant [37], these reactions take place above 1300 °C. Hüttinger and Nill [38] indicate that the reaction of silica with C begins at 800 °C. This affirmation is however not supported on experimental evidence or a literature reference. Interactions between SiO_2 and AAEM to form silicates can also influence TPD spectra as these reactions take place with CO_2 release [28,31,39]. Calcium silicates form after $CaCO_3$ decomposition to CaO at temperatures above 650 °C [28]. Potassium silicate formation takes place via reaction of K_2CO_3 with SiO_2 at temperatures as low as 600 °C [31,40]. Thermodynamic calculations made by Anicic et al. [39] indicate that at molar ratios SiO_2:K_2CO_3 below 1:1 the presence of CO_2 exerts a high inhibiting influence, so that almost 50% of the original K_2CO_3 remains in equilibrium without decomposition.

Mg- and Na- compounds are present in much smaller quantities as Ca- and K-compounds in biomass ash so it is expected that their influence in TPD signals is of minor importance. Their decomposition should follow similar pathways as for Ca (Group IA) and K (Group IIA), respectively. $MgCO_3$ undergoes thermal decomposition at low temperatures between 113 °C and 550 °C [41]; Na_2CO_3 decomposes above 1000 °C. In presence of SiO_2 sodium silicate is formed (with CO_2 evolution) at temperatures as low as 800 °C [42]. The reaction of Na_2CO_3 with carbon resulting in CO evolution takes place at temperatures above 800 °C [43].

The presence of Fe can also influence TPD spectra. After gasification, due to reaction of Fe with CO_2, it is present as FeO in the char ash. During TPD in presence of C the oxide is reduced with CO evolution at temperatures over 700 °C [44]. Kyotani et al. [8] identified Fe_3O_4 as the

predominant Fe compound in coal char during gasification with H_2O. They conclude that during TPD it is reduced to FeO in the presence of C producing CO. This reaction takes place at temperatures higher than 750 °C. Al_2O_3 is stable a temperatures lower than 1000 °C so it is expected that this component do not exert any influence in the TPD signals [45].

2.2.2. Decomposition of biomass char ash

Few studies deal with the decomposition behavior of biomass char ash. Li et al. [46] studied the thermal decomposition of raw biomass ash and artificial mixtures representative for biomass ashes by TGA under air atmosphere. They divided the mass loss in three temperature stages: low temperature between 70 °C and 250 °C, moderate temperature between 350 °C and 450 °C and high temperature between 600 °C and 1100 °C. Mass loss of artificial mixtures at low and high temperature stages are attributed to the presence of K_2O, whereas mass loss in the low temperature range is attributed to dehydration of the alkali oxide. Mass loss at the moderate temperature stage is attributed to the presence of CaO. Raw biomass ash did not show mass loss at moderate temperatures, which they ascribe to the combination of CaO to other Ca compounds having different decomposition temperatures. According to Arvelakis et al. [31] below 800 °C, weight loss of biomass ash during heating in nitrogen is due to $CaCO_3$ decomposition according to (R6). Between 850 °C and 1150 °C, K_2CO_3 reacts with SiO_2 yielding CO_2 and above 1150 °C, mass loss is attributed to decomposition of K_2CO_3 according to (R8).

3. Materials and methods

3.1. Characterization of raw material

3.1.1. Biomass char

In the present work a high temperature char (WC1600) produced from a bark-less beech wood is used. The biomass was milled and pyrolyzed in two steps up to 500 °C and 1600 °C, respectively. Thereafter, the char obtained was sieved to a 50–100 μm fraction. Carbon content of the char amounts to 97.4 wt-% daf and ash content to 6.68 wt-% d. Ash composition analysis of WC1600 determined by inductively coupled plasma optical emission spectrometry (ICP-OES) is presented in Table 1. Cl and S were below detection limits. A detailed description of the production procedure and its characterization is presented in part 1 of the present study [6].

3.1.2. Impregnated activated carbon

The behavior of the main ash components of WC1600 (K and Ca) is investigated with a commercially available activated carbon (AC1) having ash content lower than 1 wt-% (Merck CAS 7440-44-0, particle diameter < 100 μm, BET specific surface area 740 m^2/g). AC1 was impregnated with calcium nitrate (AC1Ca) and potassium nitrate (AC1K), the ash concentration was determined by ICP-OES. For impregnation, a round bottom flask was filled with 5 g of AC1 and the correspondent solution of metal salt in demineralized water. Subsequently, the flask was attached to a vacuum rotary evaporator (Heidolph VV 2000). The flask was lowered into a water bath, which was tempered at 55 °C, and rotated with 30 min^{-1}. Using a vacuum pump, the pressure was decreased to 170 mbar. After approx. four hours, the liquid was completely evaporated. Finally, the impregnated char was dried for 12 h at 105 °C. Values for Ca, K and Si concentration for the raw activated carbon material and the two impregnated samples are given in Table 1.

Table 1
Ca, K and Si mass fractions of WC1600, raw activated carbon (AC1) and the two impregnated samples AC1Ca and AC1K measured by ICP-OES.

Sample	Ca mg/g_C	K mg/g_C	Si mg/g_C
WC1600	26.19	2.94	6.01
AC1	0.80	0.69	2.81
AC1Ca	26.45	0.69	2.81
AC1K	0.80	25.02	2.81

3.2. Experimental

The detailed experimental set-up and procedure, as well as the approach used for the correction of the TPD signals are presented in detail in section 3 of part 1 of the present study [6]. Summarizing, WC1600 is partially gasified in 80 vol-% CO_2 in Ar at 820 °C up to carbon conversion degrees of 0.25, 0.50, 0.75, 0.90 and 1. After gasification, the samples were cooled to 200 °C either in reaction atmosphere or in Ar atmosphere. Subsequently, a TPD under Ar at 3 K/min until 900 °C is performed. As proposed by Lizzio et al. [5] by cooling in Ar atmosphere the amount of stable surface complexes formed in the gasification reaction can be determined from the released CO_2 and CO during the TPD step. The obtained volume fractions using this procedure are noted as $y_{CO_2,stable}$ and $y_{CO,stable}$. If the cooling step is performed in CO_2 atmosphere, the amount of total complexes (stable and unstable) is measured. Volume fractions obtained using this procedure are called $y_{CO_2,total}$ and $y_{CO,total}$.

The impregnated activated carbon samples AC1Ca and AC1K were gasified to a conversion degree of 20% using 80 vol-% CO_2 in Ar at 800 °C. The samples were then cooled to 200 °C in a CO_2 atmosphere followed by TPD until a final temperature of 900 °C, with a heating rate of 3 K/min and flow of Ar 100 ml/min (same parameters used by the WC1600 samples). As cooling is performed under reaction atmosphere evolved CO_2 and CO are assigned as $y_{CO_2,total}$ and $y_{CO,total}$.

3.3. Data analysis

3.3.1. Determination of released CO and CO_2 amounts and calculation of the quantity of reactive sites

The determination of the CO and CO_2 amounts released during the TPD experiments and the calculation of the quantity of reactive sites is performed according to the procedure described in section 3.4 of Part 1 of the present study [6] (Eq. numbers refer to Part 1). Volume fractions of Ar ($y_{Ar}(t)$), CO_2 ($y_{CO_2}(t)$) and CO ($y_{CO}(t)$) are calculated from the ion current signals of the mass spectrometer using Eq. (3) to (6). With these values, the molar flows of CO_2 and CO are calculated using Eq. (11). The amount of desorbed gas species n_{CO} and n_{CO_2} is determined by integration of the molar flows using Eq. (12) and the determination of the total quantity of reactive sites is performed by applying Eq. (13).

3.3.2. Determination of the maximal theoretical amounts of released CO_2 and CO from the initial ash content

Theoretical maximum amounts of released CO_2 and CO originated from ash decomposition reactions can be deduced from the initial content of the corresponding inorganic element in ash presented in Table 1, and the stoichiometry of the reactions presented in Section 2.2. As an example, maximal theoretical CO_2 evolution of sample AC1Ca due to the thermal decomposition of $CaCO_3$ (R6) is calculated as follows: First, the maximal available amount of calcium carbonate is determined from the Ca content of the sample assuming that all Ca forms the carbonate. Then, the corresponding amount of CO_2 that evolves according to (R6) is determined. The same procedure is used for each reaction considered in chapter 4.

4. Results and discussion

4.1. CO and CO_2 release during TPD of AC1Ca and AC1K

CO_2 and CO signals during TPD of AC1Ca and AC1K are depicted in

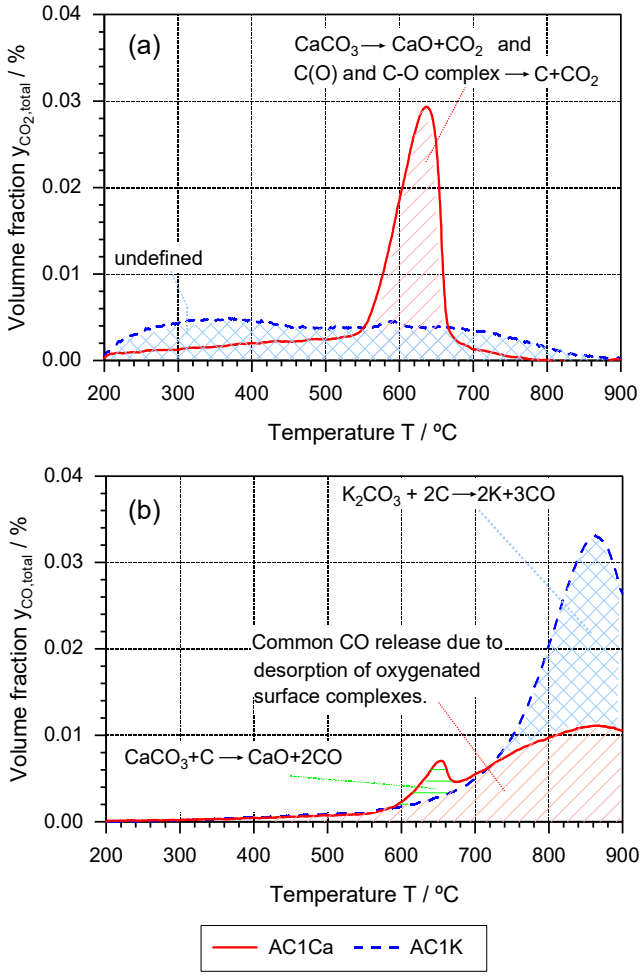

Fig. 2. TPD spectra during determination of total surface complexes for the impregnated activated carbon samples AC1Ca and AC1K submitted to gasification at 800 °C and 80 vol-% CO_2 until 20% carbon conversion. The cooling step before TPD is performed under CO_2 atmosphere. (a) CO_2 and (b) CO release.

Fig. 2. Table 2 presents a comparison between experimental amounts of released CO_2 and CO and the maximal theoretical values that can be calculated from the samples according to their initial ash composition and to selected decomposition reactions using the methodology presented in Section 3.3.2.

The CO_2 spectrum of sample AC1Ca, presented in Fig. 2(a), shows a pronounced peak at 630 °C that does not appear in the sample AC1K. Thus, its formation can be attributed in part to the decomposition of $CaCO_3$ according to (R6). As presented in Section 2.2.1 under TPD conditions this reaction is favored over reaction (R7) and takes place in the temperature interval at which this peak appears. The presence of $CaCO_3$ in the sample after cooling can be explained as follows: During gasification, $CaCO_3$ undergoes continuous decomposition, according to (R7), and formation, according to reverse reaction of (R6). The latter is favoured due to the presence of CO_2. This sequence is proposed to be the mechanism responsible of the catalytic effect exerted by the presence of Ca during gasification [29]. By cooling in CO_2, all CaO forms the carbonate and due to the lower temperatures, its decomposition is stopped. Therefore, Ca is present as its carbonate $CaCO_3$ in the sample at 200 °C. During the following TPD, the carbonate decomposes according to (R6) yielding CO_2 in the gas phase. Row A.1 of Table 2 shows the calculated amount of CO_2 that might be released from the sample as a result of $CaCO_3$ decomposition according to (R6) using the initial Ca content in the ash. In row A.2 of the same table the experimentally released CO_2 during TPD, indicated with diagonal hatch pattern on Fig. 2a, is presented. The higher value of the experimental CO_2 amount indicates the presence of oxygenated surface complexes, such as carboxylic anhydride and lactone groups, that are formed during gasification and desorb in this temperature interval [10,13]. In the present case, the desorbed oxygenated surface complexes correspond to the sum of stable and unstable complexes as cooling was performed under CO_2 atmosphere (for a detailed explanation of the experimental procedure refer to section 3.3 of part 1 of the present study [6]). The calculated amount of desorbed CO_2, following the procedure of section 3.3.2, constitutes the maximum CO_2 evolution from $CaCO_3$ decomposition that can arise from the sample as it is assumed that all Ca is available for the formation of the carbonate. The true CO_2 amount will however be lower as it depends on the availability of Ca on the surface to undergo $CaCO_3$ formation and decomposition during TPD. Moreover, Ca availability is directly related to the amount that is catalytically active during gasification since the amount of carbonate that undergoes the decomposition-formation mechanism during gasification is the one that decomposes during subsequent TPD [8]. Availability of Ca depends on Ca dispersion in the sample and the occurrence of sintering during gasification [8,24,47].

As can be seen from the CO_2 release of sample AC1K presented in Fig. 2(a), the presence of potassium exerts an influence on this signal in the whole temperature range. No evidence on decomposition of K-compounds on ash yielding CO_2 or CO at temperatures lower than 600 °C was found in literature. Thermal decomposition of K_2CO_3 according to (R8) takes place at temperatures higher than 900 °C so the occurrence of this reaction is improbable at the conditions used in the present work. A source of CO_2 from the K containing sample at temperatures above 600 °C can arise from the formation of potassium silicate. However, the released CO_2 would be negligible due to the low Si content of the sample. This can be supported by calculating the maximal CO_2 amount that evolves from the initial Si content in the sample (see Table 1) and reaction of SiO_2 with K_2CO_3 to form $K_2O(SiO_2)$ and CO_2. Applying the procedure depicted in Section 3.3.2, the calculated value corresponds to only 0.89% of the total experimentally released

Table 2
Calculated and experimental CO_2 and CO amounts according to proposed decomposition reactions during TPD of samples AC1Ca and AC1K.

		Released mass of gas species during TPD per initial carbon mass $mg_i/g_{c,0}$
A	**CO_2 evolution attributed to $CaCO_3$ = CaO + CO_2**	
A.1	Calculated from the initial Ca content of sample AC1Ca and the stoichiometry of the reaction.	29.04
A.2	Experimental value from TPD of sample AC1Ca (area identified with diagonal hatch pattern of Fig. 2a).	39.35
B	**CO evolution according to K_2CO_3 + 2C = 2 K + 3 CO**	
B.1	Calculated from initial K content of sample AC1K and the stoichiometry of the reaction.	26.88
B.2	Experimental value from TPD of sample AC1K (calculated as the sum of the areas marked with cross hatch pattern and diagonal hatch pattern on Fig. 2b).	63.72
B.3	Experimental value from TPD of sample AC1K minus common CO evolution (area identified with diagonal hatch pattern on Fig. 2b).	30.32

CO_2 determined from the cross hatched area of Fig. 2. A similar behavior in the CO_2 signal is observed in the WC1600 samples analyzed in part 1 of the present study (as presented in Fig. 3 and Fig. 4 of part 1 [6]). There, it is concluded that this CO_2 release cannot be the result of desorption of oxygenated surface complexes as preheated and unconverted char samples of WC1600 show a similar CO_2 spectrum. Desorption of oxygenated surface complexes yielding CO_2 from sample AC1K is rather unlikely. The considerable amount of CO_2 that desorbs from oxygenated surface complexes from sample AC1Ca shows a possible influence of the presence of Ca in the formation of oxygen surface complexes yielding CO_2 during TPD. Finally, at approx. 590 °C the CO_2 signal of sample AC1K shows a small peak that can be the result of decomposition of $CaCO_3$ formed from the original Ca content of the sample presented in Table 1.

Fig. 2(b) shows the CO signals during TPD for both samples AC1K and AC1Ca. As expected, CO release takes place at higher temperatures than CO_2. Excluding the peak at 650 °C from sample AC1Ca, both signals seem to have the same course up to approx. 730 °C. Afterwards, the signal of the sample AC1K exhibits a faster increase until reaching a maximum at 850 °C. Enhanced CO evolution of sample AC1K after 730 °C can be attributed to decomposition of K_2CO_3 according to (R9) which predominates over the thermal decomposition following (R8) [32]. During gasification, K undergoes reactions that include a continuous decomposition and formation of the carbonate by means of (R9) and the reverse reaction of (R8). K_2O needed for the formation of the carbonate arises from reaction of elemental K with CO_2 in an intermediate step [48,49]. By stopping the gasification reaction, K is present in the sample mainly as K_2CO_3 and during cooling in CO_2 remaining K_2O reacts to K_2CO_3 according to the reverse reaction of (R8). At 200 °C, catalytically active K, or the one that undergoes K_2CO_3 formation and decomposition, is present in the sample as K_2CO_3. During subsequent heating at TPD conditions, the carbonate decomposes following (R9). Table 2 section B shows the calculated CO amount that arises from (R9) using the initial K content of the impregnated sample (row B.1) and the CO released during the experiment using two approaches (row B.2 and row B.3). Row B.2 includes the whole CO amount released from sample AC1K (sum of areas indicated with cross and diagonal hatched patterns on Fig. 2(b)). In Row B.3 the value of the additional CO evolution of sample AC1K over sample AC1Ca is shown (area of the cross-hatched pattern on Fig. 2(b)). The obtained experimental value presented in row 3 is close to the calculated value from the initial K content of the sample. Consequently, it can be stated that the CO curve of the sample AC1K results from two contributions: One that is common for both samples, and therefore independent of impregnation, and other that originates from the decomposition of K_2CO_3 present in the sample. CO evolution due to decomposition of K_2CO_3 amounts to 42% of the total evolved CO of sample AC1K.

Regarding the common CO evolution, as the original ash content of the samples is very small (< 1 wt-%), decomposition reactions of common ash components should not have a relevant influence on the CO signal. Si present in both samples (see Table 2) which is typically present as silicon oxide, decomposes in presence of C at high temperatures (1300 °C) [36,37]. Moreover, it would rather tend to form calcium or potassium silicates with CO_2 evolution at lower temperatures [28,31]. K present in the sample AC1Ca could also be a source of CO through K_2CO_3 decomposition. However, the calculated amount of CO that would evolve using the initial K content of the sample and (R9) amounts to only 1,26% of the total area marked with diagonal hatch pattern of Fig. 2(b). The common CO release should then be the result of desorption of oxygenated complexes yielding CO like phenols, carbonyl/quinones and ether groups that are formed on the samples during gasification. The presence of a high amount of oxygenated complexes yielding CO is related to a sample having a high amount of micropores [16] which should be the case of the activated carbon samples used in the present work.

Finally, the origin of the CO peak at 650 °C of the sample AC1Ca (identified with horizontal hatch pattern in Fig. 2(b)) can be associated with the decomposition of $CaCO_3$ in presence of C according to (R7). This reaction takes place to a smaller extent than thermal decomposition of $CaCO_3$ [29]. The mass of CO released calculated by this peak area amounts to 2,11 $g_{CO}/g_{C,0}$. Based on the stoichiometry of reaction (R7) it is calculated that this amount would be released from an initial Ca content of 1,51 $mg/g_{C,0}$ which represents 5,7% of the Ca present in the sample. Another possible origin is the desorption of carboxylic anhydride that, as shown in Fig. 1, decomposes yielding CO and CO_2 in the temperature interval in which this peak appears (shifted to the higher temperatures). However, as the occurrence of this peak depends on the presence of Ca in the sample the most likely cause of its appearance is the decomposition according to (R7).

From the previous analysis, it can be concluded that the presence of Ca and K in samples of partially gasified activated carbon exerts a big influence on the CO_2 and CO spectra obtained during subsequent TPD. CO_2 and CO release is the result of a combination of desorption of oxygenated surface complexes and decomposition reactions of carbonates of Ca and K. Both are formed during gasification under CO_2 atmosphere and participate in the gasification reaction. TPD spectra can be interpreted as follows:

- The peak of the CO_2 signal of the sample impregnated with Ca (AC1Ca) is in its major fraction the result of decomposition of $CaCO_3$ according to (R6). Extra CO_2 evolution can be attributed to decomposition of oxygen surface complexes followed by desorption of CO_2.
- CO evolution at temperatures higher than 700 °C for sample AC1K results from decomposition of K_2CO_3 (according to (R9)) and decomposition of oxygen surface complexes followed by desorption of CO.
- Regardless of impregnation, CO release shows for both samples (AC1K and AC1Ca) a common course. This release is attributed to decomposition of oxygenated surface complexes formed during gasification followed by desorption of CO.
- CO_2 release does not exhibit a common course comparing both samples. Moreover, sample AC1K does not show a CO_2 signal arising from decomposition of oxygenated surface complexes. Consequently, formation of oxygenated surface complexes yielding CO_2 seems to be promoted by the presence of Ca in the sample.
- Decomposition of $CaCO_3$ in presence of C according to (R7) takes place to a smaller extent than thermal decomposition (R6) giving a peak in the CO spectrum of the sample AC1Ca at 650 °C.
- The presence of K exerts an influence on the CO_2 signal that could not be explained from evidence found in the literature available. The same influence was detected in samples of partially gasified WC1600 as presented in part 1 of the present study [6].

4.2. CO and CO_2 release during TPD of completely gasified WC1600

TPD profiles of ash of samples of WC1600 completely gasified ($X_C = 1$) using the procedures for determination of total and stable complexes (described in section 3.3 of part 1 of the present study [6]) are presented in Fig. 3.

CO_2 signals show the characteristic peaks at 610 °C ($y_{CO_2,total}$) and 430 °C ($y_{CO_2,stable}$) that also appear in the WC1600 samples partially gasified as presented in Figs. 3 and 4 of part 1 of the present study [6]. From the analysis of the preceding section, the origin of the peak at 610 °C can be attributed to the decomposition of $CaCO_3$ that is present in the sample after cooling in CO_2. Both CO_2 peaks of samples AC1Ca and WC1600 appear in the same temperature interval, with a small difference of 20 K. The experimental amount of CO_2 that is released from this peak amounts to 0,0092 $g_{CO2}/g_{C,0}$ while the maximal CO_2 amount that would evolve from the initial Ca content in the sample of WC1600 (reported in Table 1) following the decomposition reaction of

(R6) increases to 0,033 $g_{CO2}/g_{C,0}$. This result indicates that only a fraction of Ca in ash of WC1600 is capable to undergo $CaCO_3$ decomposition. As stated above, this fraction corresponds to the quantity of Ca that is catalytically active during the gasification process as it is able to undergo formation and decomposition of $CaCO_3$ at gasification conditions. As reported by Radovic et al. [47] and Cazorla-Amorós et al. [24] the catalytic activity of the metal during gasification is dependent on Ca-dispersion in the sample. Non-active Ca may be sintered in the matrix of the ash sample [24].

When the procedure for determination of stable complexes is applied, the CO_2 atmosphere is changed to Ar at gasification temperature after reaching the desired carbon conversion degree. Consequently, recombination of CaO (originated from decomposition of $CaCO_3$ following the decomposition and formation mechanism responsible for the catalytic influence exerted by Ca on the gasification reaction with CO_2) to form $CaCO_3$ does not take place. Moreover, remaining $CaCO_3$ decomposes to CaO and CO_2 at gasification temperature. After cooling, the amount of Ca that participates in the gasification reaction is present as CaO and consequently, during the subsequent TPD, the peak at 600 °C does not appear. The CO_2 peak at 430 °C observed in Fig. 3 must originate from a compound whose formation is inhibited by the presence of CO_2 during cooling, as this peak does not appear in the signal of $y_{CO_2,total}$. From the literature review, only Mg compounds decompose at temperatures lower than 500 °C but yield CO_2 instead of CO [41]. Hall and Calo [16] obtained a similar CO_2 peak centered at 427 °C in their TPD studies of oxidized coal char. However, no indication about the origin of this peak is given. A possibility arises from desorption of chemisorbed CO_2 on CaO. Linares-Solano et al. [50] pointed out that, at temperatures lower than 300 °C, CO_2 chemisorption on CaO predominates over the carbonation reaction (reverse reaction of (R6)). Considering the experimental conditions used in the present work, as the atmosphere is changed at gasification temperature from CO_2 to Ar, all $CaCO_3$ should decompose to CaO with CO_2 release. It is possible that during the rapid cooling a small amount of CO_2 remains chemisorbed on the sample and is later desorbed during the subsequent TPD. This aspect should be further investigated.

Another possible source of CO_2 during TPD is the formation of potassium silicate. However, no CO_2 is detected in the temperature range at which this reaction takes place (above 650 °C) so its occurrence is unlikely. Finally none of the CO_2 signals show the continuous evolution in the whole temperature interval that appears in the partially gasified samples of WC1600 (see Fig. 3 and Fig. 4 of part 1 of the present study [6]) and the sample AC1K (see Fig. 3). Thus, the presence of C in the sample must have an influence on the event that causes the appearance of this signal.

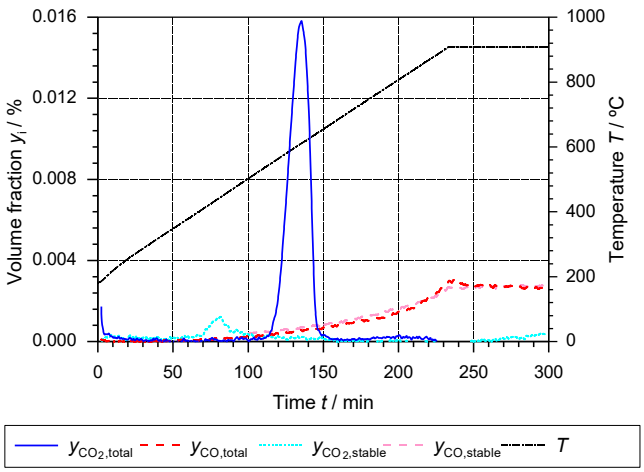

Fig. 3. CO_2 and CO release during TPD for determination of surface complexes for ash of WC1600 submitted to total gasification at 820 °C and 80 vol-% CO_2.

CO signals of both $y_{CO,total}$ and $y_{CO,stable}$ show the same course as the one obtained from blank experiments indicating that no decomposition of ash components yielding CO takes place. The present results confirm that K_2CO_3 decomposition in the studied temperature range takes only place in presence of C according to (R9). Moreover, no thermal decomposition of K_2CO_3 according to (R8) occurs as no CO_2 is detected in the high temperature region. As reported in the literature this reaction takes place at temperatures higher than 900 °C [30].

From the above presented results on TPD of ash remaining after gasification of WC1600 with CO_2 it can be stated that:

- Only a fraction of Ca present in ash of WC1600 undergoes $CaCO_3$ decomposition. This fraction is related to the quantity of Ca that is catalytically active during CO_2 gasification.
- After cooling in Ar atmosphere Ca in ash of WC1600 is present as CaO. Consequently during TPD the pronounced peak at approx. 600 °C, attributed to $CaCO_3$ decomposition, does not appear.
- Chemisorbed CO_2 on CaO can be the source of the small peak at approx. 430 °C of the signal of stable complexes $y_{CO_2,stable}$.
- Contrary to the results on the partially gasified samples, a release of CO_2 at low temperatures does not take place. Consequently, release of CO_2 at low temperatures depends on the presence of C in the sample.
- Decomposition of ash components yielding CO does not take place during TPD of ash obtained after total gasification of WC1600.

4.3. Comparison of spectra from ash and partially gasified samples of WC1600

Based on the conclusions about the course of the CO_2 and CO signals during TPD obtained so far an attempt is made to identify the contributions of both ash decomposition reactions and desorption of oxygen surface complexes during TPD of WC1600 samples partially gasified in CO_2 atmosphere. The results for these samples obtained for 0.25, 0.50, 0.75 and 0.90 carbon conversion degrees are presented in detail in part 1 of the present study [6].

Regarding Figs. 3 and 4 of part 1 of the present study [6], CO_2 signals of total surface complexes are dominated by the pronounced peak at 600 °C that is characteristic for $CaCO_3$ decomposition. The peak shows small variations in height and maximum peak temperature. The CO_2 signal of stable complexes is characterized by the peak at 430 °C possibly due to chemisorbed CO_2. Additionally to these characteristic peaks the course of the CO_2 signals of both total ($y_{CO_2,total}$) and stable ($y_{CO_2,stable}$) complexes show a common behavior that extends over the whole temperature range studied. It can be identified by overlapping the signals of $y_{CO_2,total}$ and $y_{CO_2,stable}$ as shown in Fig. 3 of part 1 of the present study [6]. As the signal is common for both stable and total complexes it should evolve from a compound that remains stable at gasification conditions and consequently does not participate in the gasification reaction. As shown in Fig. 4(a), it corresponds to the signal of $y_{CO_2,stable}$ without the peak at 430 °C. Latter is taken from the signal of stable CO_2 ($y_{CO_2,stable}$) of the sample completely gasified ($X_C = 1$) presented in Fig. 3. It has been shown that the common CO_2 release is not caused by desorption of oxygen surface complexes as it appears on degassed samples that have not been submitted to partial gasification. From the analysis presented in sections 4.1 and 4.2, it is also concluded that it emerges during TPD when C and K are present in the sample.

A detailed analysis of the CO_2 signals of the samples gasified up to $X_C = 0.90$ carbon conversion degree (both stable and total CO_2) show a deviation to higher values starting from approx. 650 °C onwards compared to the common CO_2 course. This can be seen in detail in Fig. 4(b) where the area corresponding to the additional CO_2 (hatched area) and the course of this additional release (dashed line) show a peak at approx. 820 °C. At the same time, the CO signals show a steep increase (see $X_c = 0.90$ in Fig. 4(a) and (b) of part 1 of the present study [6]),

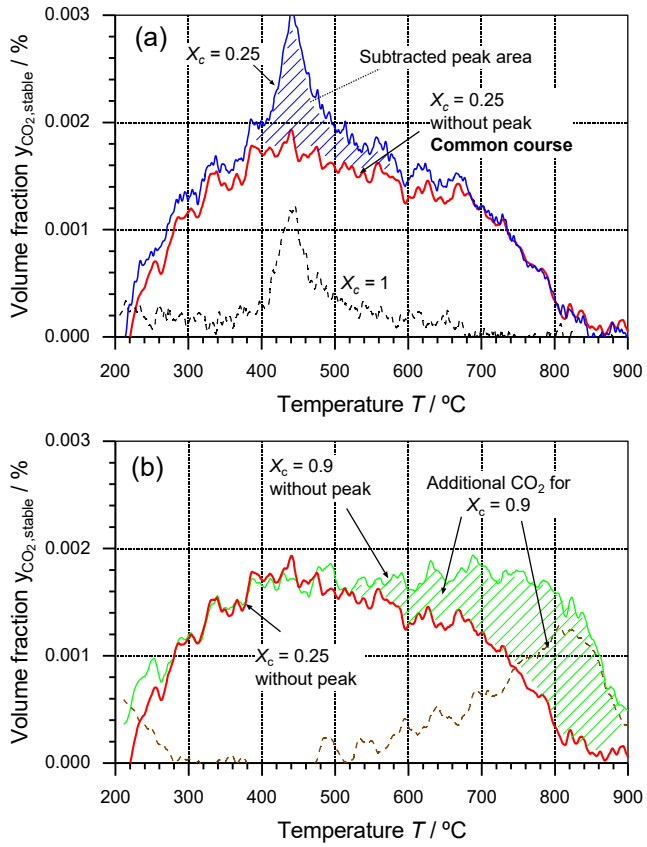

Fig. 4. CO_2 evolution during TPD for determination of stable surface complexes for ash of WC1600, gasification at 820 °C and 80 vol-% CO_2. (a) Graphical determination of common course of the CO_2 signal. (b) Graphical determination of additional CO_2 release at X_C = 0.90.

compared to the signals obtained at X_c = 75%. At X_c = 0.90, released CO values are the highest of all conversion degrees. This behavior is contrary to that observed from 25% to 75% conversion where the CO signal is shifted towards lower values. The enhanced CO_2 and CO evolution at 90% conversion may be explained by the initial structure of WC1600 and its development during gasification. Due to the high temperature at which the sample was pyrolyzed (1600 °C), the graphitic structure of WC1600 became highly ordered so that places for the formation of oxygenated surface complexes are limited [12]. Thus, the gasification reaction is predominantly caused by the catalytic influence exerted by the main ash components Ca and K. At high conversion degrees (X_c = 0.90) collapsing of the carbon structure gives rise to the formation of edges and imperfections on the basal planes of the graphite layers were formation of oxygenated surface complexes is favored. It would be expected that in some point at a conversion degree higher than X_c = 0.90 further collapsing of the char matrix occurs and the amount of surface complexes declines rapidly until reaching total conversion. Based on the decomposition temperatures of oxygenated surface complexes presented in Fig. 1, the origin of these newly formed complexes that are released as CO_2 cannot be fully explained as CO_2 evolution usually does not take place at temperatures higher than 700 °C. A possible source of this CO_2 evolution is the occurrence of a secondary reaction within the pores of the sample between released CO and the surface of the carbon [16], as presented in the literature review.

CO release of the samples of WC1600 obtained using the procedure for determination of total complexes ($y_{CO,total}$) (Fig. 4(b) of part 1 of the present study [6]), show a similar course as the CO signal of sample AC1K (Fig. 3(b)). These samples were cooled under CO_2 atmosphere. Consequently, as presented in section 4.1, the CO signal is the result of decomposition of K_2CO_3 according to (R9) and desorption of oxygenated surface complexes (stable and unstable). The tendency of the CO signal towards lower values as the conversion is increased from X_c = 0.25 to X_c = 0.75 can be ascribed to the tendency of K to volatize during gasification, as reported by several authors [22,23,32]. Another possible explanation for this behavior is a reduction in the amount of C that is available for K_2CO_3 decomposition with an increment in the carbon conversion. The steep increase in CO evolution at X_c = 0.90 is due to an enhanced formation of active sites in the structure of the carbon matrix at high conversion degrees. When CO_2 is changed to Ar at gasification temperature, (R9) takes place until all K_2CO_3 has decomposed to K and CO and new formation of the carbonate does not occur. Consequently, CO evolution is not affected by K_2CO_3 decomposition and should be then the product of the sole decomposition of oxygenated surface complexes followed by desorption of CO. Additionally, as shown in Fig. 4(a) of part 1 of the present study [6], the CO signals of these samples ($y_{CO,stable}$) show a similar behavior as the one obtained for $y_{CO,total}$ in which the curves are shifted to lower values of CO as the conversion degree increases from X_c = 0.25 to X_c = 0.75. Therefore, although the CO signal of $y_{CO,stable}$ is not affected by decomposition of K_2CO_3 its presence during gasification exerts an influence on the formation of active sites that remain stable during gasification.

4.4. Quantification of catalytically active and reactive sites during gasification of WC1600

Following the procedure for the determination of reactive sites proposed by Lizzio et al. [5], $y_{CO_2,stable}$ and $y_{CO,stable}$ are subtracted from $y_{CO_2,total}$ and $y_{CO,total}$ at each conversion degree (for $y_{CO_2,stable}$ the peak at 430 °C is excluded from the calculation as shown in Fig. 5(a)). As the results are influenced by the presence of ash in the samples, they are not only representative for the amount of reactive sites participating in the gasification reaction. Moreover, $y_{CO_2,total}$ and $y_{CO,total}$ include the amounts of CO_2 and CO that evolve when Ca and K undergo the conversion mechanisms that are responsible for their catalytic influence during gasification. Consequently, the CO_2 and CO spectra obtained following the procedure proposed by Lizzio et al. [5] in the present work are a measure for reactive sites and catalytically active sites representing the amount of K and Ca in ash that exerts a catalytic influence during gasification with CO_2.

The course of the obtained CO_2 signal for each conversion degree is presented in Fig. 5(a) together with the CO_2 signal of ash of the completely gasified sample (X_c = 1). In this figure, the strong influence of the presence of Ca in the TPD signal, and consequently during gasification, is noticeable as the peaks are very similar to that of the sample at X_c = 1. Moreover, as conversion increases the course of the signals tends to be similar to the one at X_c = 1. Contrary to the tendency of K to volatilize, Ca remains in the char during gasification [32]. Assuming that the catalytically active Ca remains constant during gasification it can be quantified by the amount of desorbed CO_2 of the sample completely gasified (X_c = 1) when cooling is performed in CO_2. Fig. 6(a) shows the calculated CO_2 amounts released from reactive plus catalytically active sites (bars marked with diagonal hatch pattern) obtained from the curves presented in Fig. 5(a). The calculated amounts for all conversion degrees (X_c = 0.25 to X_c = 0.90) are higher than the CO_2 amount released at X_c = 1. Extra CO_2 in samples partially gasified indicates that reactive sites participate in the gasification reaction. These reactive sites form oxygenated surface complexes, such as, lactone, peroxide or carboxylic anhydride that decompose and desorb as CO_2 in a similar temperature interval at which $CaCO_3$ decomposition takes place (as can be seen in Fig. 1). As shown in Fig. 6(a), the calculated extra CO_2 evolution is more pronounced in the early stages of gasification up to X_c = 0.5. From this conversion degree onwards, the amount of evolved CO_2 remains almost constant. Bars marked with crossed hatch pattern show the CO_2 amounts corresponding to stable

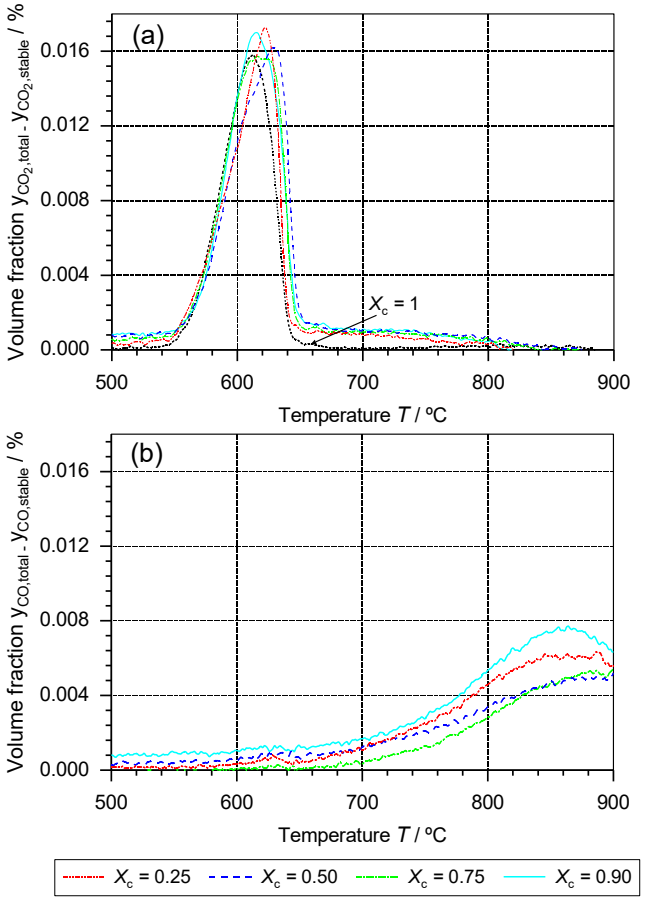

Fig. 5. TPD spectra as a function of temperature for carbon conversion degrees after partial gasification WC1600 accounting for catalytically active ash components and unstable surface complexes; a) CO_2 b) CO release.

sites. These are calculated from the CO_2 signals of Fig. 4(a) of part 1 of the present study [6] without the peak at 430 °C. The bars show a small decrease up to X_c = 0.75 followed by the increase at X_c = 0.90 attributed to the formation of oxygenated surface complexes. The slight decrease can be related to loss of K during gasification that, as stated in section 4.1, is responsible for the CO_2 evolution of the common course of the CO_2 signal.

Regarding CO, the curves presented in Fig. 5(b) show a similar course as the one obtained for total and stable complexes having a slight tendency to lower values as the conversion degree increases from X_c = 0.25 to X_c = 0.75 followed by the steep increase for the sample obtained until X_c = 0.90. In this case, it is not possible to set a baseline or to separate the contributions related to catalytically active sites due to the presence of K and reactive sites. K_2CO_3 decomposition takes place only in presence of C (according to (R9)). Consequently, oxygenated surface complexes must be present in the sample. The maximal CO amount that would evolve from K_2CO_3 decomposition using the initial K content of WC1600 presented in Table 1 and the stoichiometry of reaction of (R9) amounts to 0,0036 $g_{CO2}/g_{C,0}$. As it is the case for Ca, not all K is located on the char surface but rather in the carbon bulk of the char particle. Thus, not all K is available for carbonate formation and decomposition under gasification conditions. Moreover, the amount of K that is active during gasification can change continuously due to volatilization. However, for both CO and CO_2, the sum of the two contributions is a measure for the amount of sites on the surface of the char available for the gasification reaction. Released CO amounts corresponding to the sum of reactive sites plus catalytically active sites are calculated from the curves presented in Fig. 5(b) and presented in Fig. 6(b) (bars marked with diagonal hatch pattern). Crossed hatched bars of the same figure show the CO amounts released from stable complexes calculated from the curves presented in Fig. 4(a) of part 1 of the present study [6]. The results indicate that the ratio of reactive sites plus catalytically active sites vs. stable sites remains constant over the conversion degrees studied (see Fig. 4(b)). In the present work, the amount of reactive plus catalytically active sites for all conversion degrees studied amounts to 54% of the CO released in total. It seems reasonable to state that the presence of K has an influence in the formation of both stable and reactive surface complexes.

The amount of reactive plus catalytically active sites was calculated using Eq. 13 of part 1 of the present study [6]. The CO and CO_2 molar amounts in the bars marked with diagonal hatch pattern of Fig. 6 represent the differences of $(n_{CO,total} - n_{CO,stable})$ and $(n_{CO_2,total} - n_{CO_2,stable})$, respectively. This equation was originally defined assuming that desorbed CO and CO_2 were a measure of reactive sites only. However, as the obtained CO and CO_2 signals include the effect of decomposition and desorption of unstable surface complexes together with decomposition of catalytically active ash components, the calculated amount includes both contributions and is therefore designated as $x_{reactive+catalytic}$ in the present work.

The relation between the specific conversion rate R_m (see Eq. 1 of

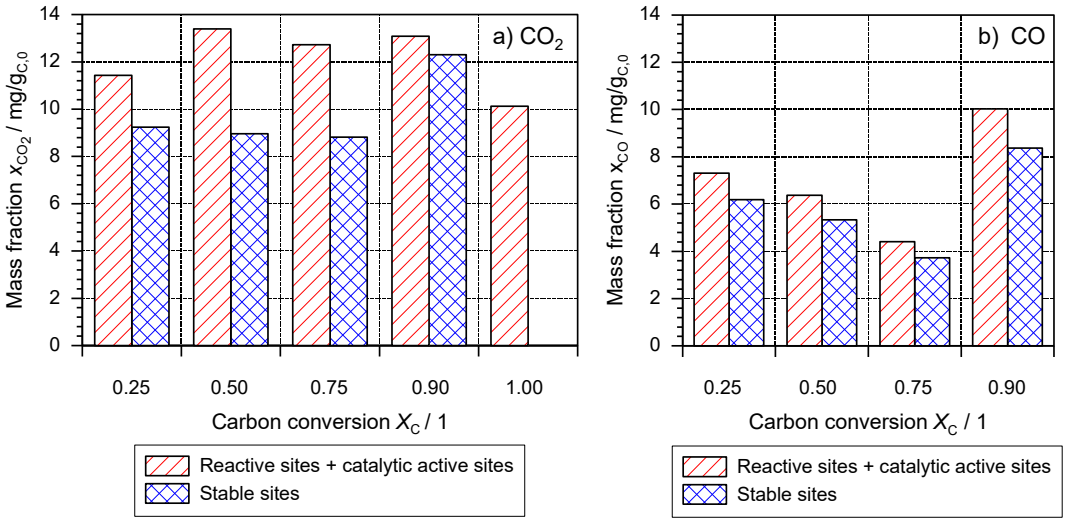

Fig. 6. CO_2 (a) and CO (b) amounts released as function of carbon conversion of WC1600 for catalytic active ash components, reactive surface complexes and stable surface complexes.

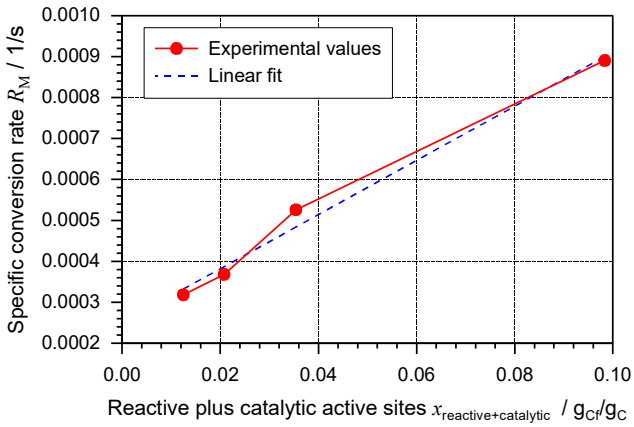

Fig. 7. Specific conversion rate vs. $x_{\text{reactive}+\text{catalytic}}$ for the gasification of WC1600 at 820 °C in 80 vol-% CO_2.

Table 3
Specific conversion rate constants k reported Lizzio et al. [5] and determined in present work. Calculated values of reactive sites using the TPD method and Eq. 1 of part 1 of the present work.

Fuel	Gasification temperature °C	k s^{-1}
Bituminous coal char [5]	820	0.003373
Saran char [5]	860	0.005947
Demineralized lignite char [5]	700	0.001366
Beech wood char (present work)	820	0.006616

part 1 [6]) and $x_{\text{reactive}+\text{catalytic}}$ (see Eq. 13 of part 1 [6]) is presented in Fig. 7. A linear correlation between R_m and $x_{\text{reactive}+\text{catalytic}}$ can be observed which is in accordance with Eq. 1 of part 1 of the present study [6]. As stated by Lizzio et al. [5], this equation implies that the surface concentration of active sites available for the gasification reaction (C_{C_f}) should be proportional to the specific conversion rate during the gasification reaction, as the specific conversion rate constant k depends only on temperature. The calculated values of $x_{\text{reactive}+\text{catalytic}}$ seem to be a quantitative measure for C_{C_f}. Moreover, this approach is able to include the effect of the catalytic influence exerted during gasification by the presence of K and Ca in ash of the sample.

Eq. (4) is an analytical expression for the linear fit of the experimental values presented in Fig. 7.

$$R_m = 0.006616\,s^{-1} x_{\text{reactive}+\text{catalytic}} + 0.000249\,s^{-1} \quad (4)$$

In conformity with Eq. 1 of part 1 of the present work [6], the slope of the linear fit (0.006616 s^{-1}) is a measure of the specific conversion rate constant k at T = 820 °C between X_C = 0.25 and X_C = 0.90. Mean values obtained by Lizzio et al. [5] using the same approach for the gasification of coal chars of different origins are presented in Table 3. As indicated in the literature review, they attempted to eliminate the influence of ash decomposition by only using the CO signal in their calculations. As shown in the table, despite the different materials the obtained values are of the same order of magnitude. However, it should be taken into account that the specific conversion rate constant k is exponentially dependent on temperature. Thus, a comparison of the values should be made with caution. For specific conversion rates lower than 0.0003 s^{-1} (or X_C < 0.25), the correlation is not proven, as the linear fit does not reach the zero value (y-intercept is 0.000249 s^{-1}).

5. Summary

During gasification of WC1600 with CO_2, three different kinds of sites on the char surface can be observed: stable and reactive sites as proposed and defined by Lizzio et al. [5] and additionally catalytically active sites which represent the influence of catalytically active components of ash. Release of CO_2 and CO during TPD of partially gasified samples of WC1600 using CO_2 as gasification agent is the result of decomposition of oxygenated surface complexes followed by desorption of the gaseous products as well as decomposition of carbonates of Ca and K. Decomposition of $CaCO_3$ is identified as the main source of CO_2 and that of K_2CO_3 as the main source of CO. The released amounts of CO_2 and CO are a measure of the catalytic influence of each metal in the gasification reaction. Moreover, the presence of Ca and K promote the creation of stable sites as well as reactive sites where oxygenated surface complexes are formed.

Due to the high pyrolysis temperature of the char investigated (WC1600), the char presumably exhibits a high grade of graphitization limiting the availability of active sites for the formation of oxygenated surface complexes. Hence, the catalytic gasification induced by Ca and K is the dominating process. Only at higher carbon conversion degrees (X_C = 0.90), an enhanced formation of both stable and reactive sites is observed.

A linear correlation between specific conversion rate R_m and the amount of reactive plus catalytically active sites is derived from the experimental data. This indicates that the calculated value is an appropriate measure of the available sites (reactive and catalytically active) on the char surface participating in the gasification reaction of WC1600 with CO_2.

Future experiments will focus on a wider range of experimental conditions in order to investigate the applicability of the correlation for the conversion rate in entrained-flow gasification. For now, the presented correlation for the conversion rate is only valid for one parameter set. Varying gasification temperature and CO_2 partial pressure is essential in order to further validate this model and extend the previous data set.

Declaration of Competing Interest

The authors declare that they have no known competing financial interests or personal relationships that could have appeared to influence the work reported in this paper.

Acknowledgments

The authors gratefully acknowledge the financial support by the Helmholtz Association of German Research Centres (HGF) in the frame of the Helmholtz Virtual Institute for Gasification Technology – HVIGasTech (VH-VI-429) and the German Academic Exchange Service (DAAD) for funding the research visits of Prof. Rincón Prat at KIT.

References

[1] Di Blasi C. Combustion and gasification rates of lignocellulosic chars. Prog Energy Combust Sci 2009;35(2):121–40. https://doi.org/10.1016/j.pecs.2008.08.001.
[2] Klose W, Wölki M. On the intrinsic reaction rate of biomass char gasification with carbon dioxide and steam. Fuel 2005;84(7):885–92. https://doi.org/10.1016/j.fuel.2004.11.016.
[3] Mahinpey N. Review of gasification fundamentals and new findings: Reactors, feedstock, and kinetic studies. Chem Eng Sci 2016;148:14–31. https://doi.org/10.1016/j.ces.2016.03.037.
[4] Irfan M, Usman M, Kusakabe K. Coal gasification in CO_2 atmosphere and its kinetics since 1948: a brief review. Energy 2011;36:12–40. https://doi.org/10.1016/j.energy.2010.10.034.
[5] Lizzio AA, Jiang H, Radovic LR. On the kinetics of carbon (Char) gasification: Reconciling models with experiments. Carbon 1990;28(1):7–19. https://doi.org/10.1016/0008-6223(90)90087-F.
[6] Schneider C, Rincon S, Kolb T. Determination of active sites during gasification of biomass char with CO_2 using temperature-programmed desorption. Part 1: Methodology & Desorption Spectra. Fuel 2019. https://doi.org/10.1016/j.fuel.2019.116726.
[7] Kyotani T, Karasawa S, Tomita A. A TPD study of coal chars in relation to the catalysis of mineral matter. Fuel 1986;65(10):1466–9. https://doi.org/10.1016/0016-2361(86)90125-0.
[8] Kyotani T, Zhang Z, Hayashi S, Tomita A. TPD study on H_2O-gasified and O_2-chemisorbed coal chars. Energy Fuels 1988;2(2):136–41. https://doi.org/10.1021/

ef00008a006.
[9] Guizani C, Jeguirim M, Gadiou R, Escudero Sanz FJ, Salvador S. Biomass char gasification by H_2O, CO_2 and their mixture: evolution of chemical, textural and structural properties of the chars. Energy 2016;112:133–45. https://doi.org/10.1016/j.energy.2016.06.065.
[10] Figueiredo JL, Pereira MFR, Freitas MMA, Órfão JJM. Characterization of Active Sites on Carbon Catalysts. Ind. Eng. Chem. Res. 2007;46(12):4110–5. doi:10.1021/ie061071v.
[11] de la Puente G, Pis JJ, Menéndez JA, Grange P. Thermal stability of oxygenated functions in activated carbons. J Anal Appl Pyrol 1997;43:125–38. https://doi.org/10.1016/S0165-2370(97)00060-0.
[12] Marsh H, Heintz E, Rodriguez-Reinoso F. Introduction to carbon techologies. Alicante: Universidad de Alicante; 1997.
[13] Szymański GS, Karpiński Z, Biniak S, Światkowski A. The effect of the gradual thermal decomposition of surface oxygen species on the chemical and catalytic properties of oxidized activated carbon. Carbon 2002;40(14):2627–39. doi:10.1016/S0008-6223(02)00188-4.
[14] Tremblay G, Vastola FJ, Walker Jr PL. Thermal desorption analysis of oxygen surface complexes on carbon. Carbon 1978;16(1):35–9.
[15] Figueiredo, JL, Pereira MFR, Freitas MMA, Órfao JJM. Modification of the surface chemistry of activated carbons. Carbon 1999;37(9):1379–89. doi:10.1016/S0008-6223(98)00333-9.
[16] Hall P, Calo J. Secondary interactions upon thermal desorption of surface oxydes from coal chars. Energy Fuels 1989;3(3):370–6. https://doi.org/10.1021/ef00015a020.
[17] Boehm HP. Surface oxides on carbon and their analysis: a critical assessment. Carbon 2002;40(2):145–9. https://doi.org/10.1016/S0008-6223(01)00165-8.
[18] Zhou JH, Sui ZJ, Zhu J, Li P, Chen D, Dai YC, et al. Characterization of surface oxygen complexes on carbon nanofibers by TPD, XPS and FT-IR. Carbon 2007;45(4):785–96. https://doi.org/10.1016/j.carbon.2006.11.019.
[19] Kundu S, Wang Y, Muhler M. Thermal stability and reducibility of oxygen-containing functional groups on multiwalled carbon nanotube surfaces: a quantitative high-resolution XPS and TPD/TPR study. J Phys Chem C 2008;112(43):16869–78. https://doi.org/10.1021/jp804413a.
[20] Ishii T, Kyotani T. Temperature Programmed Desorption. In: Inagaki M, Kang F, editors. Materials Science and Engineering of Carbon: Characterization Elsevier; 2016. https://doi.org/10.1016/C2014-0-03769-0.
[21] Du C, Liu L, Qiu P. Importance of volatile AAEM species to char reactivity during volatile–char interactions. RSC Adv 2017;7(17):10397–406. https://doi.org/10.1039/C6RA27485D.
[22] Matsuoka K, Yamashita T, Kuramoto K, Suzuki Y, Takaya A, Tomita A. Transformation of alkali and alkaline earth metals in low rank coal during gasification. Fuel 2008;87(6):885–93. https://doi.org/10.1016/j.fuel.2007.05.031.
[23] Nzihou A, Stanmore B, Sharrock P. A review of catalysts for the gasification of biomass char, with some reference to coal. Energy 2013;58:305–17. https://doi.org/10.1016/j.energy.2013.05.057.
[24] Cazorla-Amoros D, Linares-Solano A, Salinas-Martinez de Lecea C, Yamashita H, Kyotani T, Tomita A, et al. XAFS and thermogravimetry study of the sintering of calcium supported on carbon. Energy Fuels 1993;7(1):139–45. https://doi.org/10.1021/ef00037a022.
[25] Mu J, Perlmutter DD. Thermal decomposition of carbonates, carboxylates, oxalates, acetates, formates, and hydroxides. Thermochim Acta 1981;49(2):207–18. https://doi.org/10.1016/0040-6031(81)80175-X.
[26] Rodriguez-Navarro C, Ruiz-Agudo E, Luque A, Rodriguez-Navarro AB, Ortega-Huertas M. Thermal decomposition of calcite: Mechanisms of formation and textural evolution of CaO nanocrystals. Am Miner 2009;94(4):578–93. https://doi.org/10.2138/am.2009.3021.
[27] Dollimore D, Tong P, Alexander KS. The kinetic interpretation of the decomposition of calcium carbonate by use of relationships other than the Arrhenius equation. Thermochim Acta 1996;282–283:13–27. https://doi.org/10.1016/0040-6031(95)02810-2.
[28] Sinkó K, Pöppl M, Gábor M, Migály B. Study of the binary $CaCO_3$-SiO_2 system by quantitative DTA. J Therm Anal 1988;33(3):1003–11. https://doi.org/10.1007/BF02138623.
[29] McKee DW. Catalytic effects of alkaline earth carbonates in the carbon-carbon dioxide reaction. Fuel 1980;59(5):308–14. https://doi.org/10.1016/0016-2361(80)90215-X.
[30] Lehman RL, Gentry JS, Glumac NG. Thermal stability of potassium carbonate near its melting point. Thermochim Acta 1998;316(1):1–9. https://doi.org/10.1016/S0040-6031(98)00289-5.
[31] Arvelakis S, Jensen PA, Dam-Johansen K. Simultaneous thermal analysis (STA) on ash from high-alkali biomass. Energy Fuels 2004;18(4):1066–76. https://doi.org/10.1021/ef034065+.
[32] Kopyscinski J, Rahman M, Gupta R, Mims CA, Hill JM. K_2CO_3 catalyzed CO_2 gasification of ash-free coal. Interactions of the catalyst with carbon in N_2 and CO_2 atmosphere. Fuel 2014;117:1181–9. https://doi.org/10.1016/j.fuel.2013.07.030.
[33] Hyatt EP, Cutler IB, Wadsworth ME. Calcium carbonate decomposition in carbon dioxide atmosphere. J Am Ceram Soc 1958;41(2):70–4. https://doi.org/10.1111/j.1151-2916.1958.tb13521.x.
[34] Brown I. Thermodynamic modelling of reactions in materials chemistry. Chemistry in New Zealand 2014.
[35] Zhao H, Xu W, Song Q, Zhuo J, Yao Q. Effect of steam and SiO_2 on the release and transformations of K_2CO_3 and KCl during biomass thermal conversion. Energy Fuels 2018;32(9):9633–9. https://doi.org/10.1021/acs.energyfuels.8b02269.
[36] Biernacki JJ, Wotzak GP. Stoichiometry of the C + SiO_2 reaction. J Am Ceram Soc 1989;72(1):122–9. https://doi.org/10.1111/j.1151-2916.1989.tb05964.x.
[37] Henderson JB, Tant MR. A study of the kinetics of high-temperature carbon-silica reactions in ablative polymer composite. Polym Compos 1983;4:233–7. https://doi.org/10.1002/pc.750040408.
[38] Hüttinger KJ, Nill JS. A method for the determination of active sites and true activation energies in carbon gasification: (II) experimental results. Carbon 1990;28(4):457–65. https://doi.org/10.1016/0008-6223(90)90039-2.
[39] Anicic B, Lin W, Dam-Johansen K, Wu H. Agglomeration mechanism in bioass fluidized bed combustion – Reaction between potassium carbonate and silica sand. Fuel Process Technol 2018;173:182–90. https://doi.org/10.1016/j.fuproc.2017.10.005.
[40] Vassilev S, Baxter D, Andersen L. Vassileva Ch. An overview of the composition and application of biomass ash. Part 1. Phase-mineral chemical composition and classification. Fuel 2013;105:40–76.
[41] Kahn N, Dollimore D, Alexander K, Wilburn FW. The origin of the exothermic peak in the thermal decomposition of basic magnesium carbonate. Thermochim Acta 2001;367–368:321–33. https://doi.org/10.1016/S0040-6031(00)00669-9.
[42] Newkirk A, Aliferis I. Drying and decomposition of sodium carbonate. Anal Chem 1958;30(5):982–4. https://doi.org/10.1021/ac60137a031.
[43] Fox D, White A. Effect of sodium carbonate upon gasification of carbon and production of producer gas. Ind Eng Chem Res 1931;23(3):259–66. https://doi.org/10.1021/ie50255a011.
[44] Furimsky E, Sears P, Suzuki T. Iron-catalyzed gasification of char in CO_2. Energy Fuels 1988;2(5):634–9. https://doi.org/10.1021/ef00011a005.
[45] Thy P, Lesher CE, Jenkins BM. Experimental determination of high-temperature elemental losses from biomass slag. Fuel 2000;79(6):693–700. https://doi.org/10.1016/S0016-2361(99)00195-7.
[46] Li Q, Meng A, Li L, Zhou H, Zhang Y. Investigation of biomass ash thermal decomposition by thermogravimetry using raw and artificial ashes. Asia-Pac J Chem Eng 2014;9(5):726–36. https://doi.org/10.1002/apj.1817.
[47] Radović LR, Walker PL, Jenkins RG. Importance of carbon active sites in the gasification of coal chars. Fuel 1983;62(7):849–56. https://doi.org/10.1016/0016-2361(83)90041-8.
[48] McKee DW. Gasification of graphite in carbon dioxide and water vapor – the catalytic effects of alkali metal salts. Carbon 1982;20(1):59–66. https://doi.org/10.1016/0008-6223(82)90075-6.
[49] Spiro C, McKee D, Kosky P, Lamby E. Catalytic CO_2-gasification of graphite versus coal char. Fuel 1983;62(2):180–4. https://doi.org/10.1016/0016-2361(83)90194-1.
[50] Linares-Solano A, Almela-Alarcón M. Salinas-Martínez de Lecea C. CO_2 chemisorption to characterize calcium catalyst in carbon gasification reactions. J Catal 1990;125(2):401–10. https://doi.org/10.1016/0021-9517(90)90313-9.